

# *In vivo* determination of renal stone composition with dual-energy computed tomography

**Authors:**

John-Henry Corbett<sup>1</sup>  
Werner S. Harmse<sup>1</sup>

**Affiliations:**

<sup>1</sup>Department of Clinical Imaging Sciences, University of the Free State, South Africa

**Correspondence to:**

John-Henry Corbett

**Email:**

corbettjohnhenry@gmail.com

**Postal address:**

Department of Clinical Imaging Sciences (G61), Faculty of Health Sciences, University of the Free State, 205 Nelson Mandela Drive, Bloemfontein 9300, South Africa

**Dates:**

Received: 29 Jan. 2014

Accepted: 04 Mar. 2014

Published: 11 Sept. 2014

**How to cite this article:**

Corbett J-H, Harmse WS. *In vivo* determination of renal stone composition with dual-energy computed tomography. *S Afr J Rad.* 2014;18(1); Art. #605, 5 pages. <http://dx.doi.org/10.4102/sajr.v18i1.605>

**Copyright:**

© 2014. The Authors. Licensee: AOSIS OpenJournals. This work is licensed under the Creative Commons Attribution License.

**Read online:**

Scan this QR code with your smart phone or mobile device to read online.

**Background:** Composition of renal stones influences management of patients with renal stone disease. Currently stone composition can only be analysed *ex vivo* after stone extraction or passage, but recent introduction of dual-energy computed tomography (CT) to clinical practice has raised interest in the ability of this technology to determine composition of renal stones *in vivo*.

**Objectives:** To determine renal stone composition in patients using single-source dual-energy rapid-peak kilovolt (kVp) switching CT.

**Method:** Nineteen patients with renal stones for percutaneous nephrolithotomy were evaluated with single-source dual-energy computed tomography on a Discovery CT 750HD. The Gemstone Spectral Imaging (GSI) effective atomic number ( $Z_{\text{eff}}$ ) and attenuation at 70 keV monochromatic energy were used to predict the stone composition. Infrared spectroscopy and x-ray diffraction of stones after extraction served as the reference standard.

**Results:** Two (10.5%) of the 19 stones had uric acid as major component. The other 17 (89.5%) were calcium-based stones. No statistically significant difference between the GSI  $Z_{\text{eff}}$  and calculated effective atomic number ( $Z$ ) for stone compounds was found. The GSI  $Z_{\text{eff}}$  and attenuation could differentiate between uric acid and non-uric acid stones. No differentiation between different calcium stones could be made.

**Conclusion:** Uric acid and non-uric acid renal stones can be differentiated with single-source dual-energy *in vivo*. The GSI  $Z_{\text{eff}}$  reflects the dominant material in polycrystalline stones.

## Introduction

The incidence of renal stone disease is high, with a lifetime risk in the United States of America (USA) of 6% for women and 12% for men.<sup>1</sup> Renal stone disease has not been researched extensively in Africa due to a lack of resources and facilities, and therefore no recent data on the incidence of renal stones in South Africa are available.<sup>2</sup>

Sixteen different chemical compounds can form renal stones, although most of these are rare.<sup>3</sup> Calcium oxalate (70%), calcium phosphate (20%), uric acid (8%) and cystine (2%) are the most common stone components.<sup>4</sup> Developed countries have seen an increase in the incidence of calcium oxalate stones over the last 50 years, compared to developing countries, where the percentage of uric acid and phosphate stones remains relatively high.<sup>1</sup>

Untreated renal stone disease can lead to obstruction of an infected urinary tract, which may lead to urosepsis and death. Persistent urinary obstruction may also result in renal insufficiency and end-stage renal disease. Long-term complications can include recurrent pyelonephritis and ureteric strictures.<sup>5</sup>

The chemical composition of renal stones will influence the management of patients. Firm stones (such as calcium oxalate monohydrate and cystine) may not break up at extracorporeal shock wave lithotripsy. If the chemical composition of their stones is known, these patients can be offered percutaneous nephrolithotomy (PCNL) from the start. Systemic or familial metabolic disease may lead to urolithiasis and knowledge about the stone composition can assist in the diagnosis and treatment of such a disorder. The recurrence of certain stones can be prevented by medical and dietary measures; however, such measures can only be implemented if the stone composition is known. Improved treatment decisions could be made if accurate, non-invasive methods are available to distinguish between different stone types.<sup>1,5</sup>

The three most common methods used to determine stone composition are *in vitro* x-ray diffraction, infrared spectroscopy and polarisation microscopy. These methods are costly, time consuming and can only be performed after the surgical extraction of the stones, or when the passed stones are large enough for analysis. Consequently, they generally offer no benefit to pre-operative treatment planning.<sup>1,6</sup>

Non-enhanced multidetector computed tomography (CT) of the abdomen and pelvis is the imaging examination of choice for evaluating suspected renal stone disease, offering high sensitivity and specificity.<sup>6</sup> It can also provide information about the presence and degree of the obstruction and other possible causes of the patient's symptoms. Only 45% – 59% of renal stones demonstrated with CT are visible on abdominal overview x-rays.<sup>1</sup> The utility of abdominal overview x-rays therefore remains limited in renal stone disease.<sup>5,7</sup> A combination of abdominal overview x-rays to detect radio-opaque stones and renal ultrasound to detect hydronephrosis can be used where CT resources are limited and when radiation should be kept to a minimum, such as in pregnant or paediatric patients.<sup>5,7</sup> It has been shown that renal stone characterisation with single-energy CT using the CT number (Hounsfield units [HU]) is inaccurate due to the overlap in densities, and it is thus not advisable for use in clinical practice.<sup>3,8</sup>

Dual-energy CT combines high-energy and low-energy scanning during a single acquisition. This dual-energy data provide information related to the varying responses of different x-ray energies to tissues, which allows material differentiation and elemental decomposition.<sup>6,9,10</sup> Three main technologies are available for dual-energy scanning, namely dual-source dual-detector, single-source rapid-peak kilovolt (kVp) switching single-detector, and single-source layered-detector systems.<sup>1</sup>

A number of studies have reported the ability of dual-energy CT to accurately differentiate between the major pure-stone groups *in vitro*.<sup>9,11,12</sup> Limited *in vivo* studies have proven accuracy in differentiation between uric acid and non-uric acid groups. The subclassification of non-uric acid stones is limited to cystine-containing, struvite-containing and calcium-containing stones.<sup>6,10,13</sup> To date only one publication could be located on *in vivo* renal stone characterisation using single-source rapid kVp switching dual-energy CT.<sup>10</sup>

## Method

### Study design

A prospective, descriptive clinical study involving the pre-operative *in vivo* assessment of stone composition with dual-energy CT was conducted. All stones were renal in origin. The findings were compared to *ex vivo* laboratory stone analysis after stone extraction via PCNL.

The study was conducted in the Universitas Academic Hospital Bloemfontein at the Faculty of Health Sciences of the University of the Free State (UFS). The research protocol was approved by the Ethics Committee of the Faculty of Health Sciences, UFS, and written informed consent was obtained from all participants. The study population consisted of patients booked for PCNL from January 2011 to November 2013. These patients were all diagnosed with renal stones prior to admission, but due to a long waiting list for PCNL, a repeat non-contrast renal stone CT was performed for pre-operative planning and evaluation of disease progression.

The standard non-contrast renal stone CT protocol consists of scanning from the top of the kidneys to the bottom of the bladder with 0.625 mm slice thickness and 3 mm image reconstructions in axial, sagittal and coronal planes. Once the renal stone was identified, a targeted dual-energy CT with limited field of view was performed covering the stone area.

### Computed tomography technique

The CT examinations were performed using a 64 multidetector CT single-source with fast kVp switching (Discovery CT 750HD, GE Healthcare, Milwaukee, Wisconsin). The dual-energy protocol used was Gemstone Spectral Imaging (GSI) with rotation time 0.6 s; pitch 1.375:1; detector width 20 mm; and slice thickness 1.25 mm. Milliampere was set automatically at 640 mA distributed between 80 and 140 kVp acquisitions. GSI is a feature unique to this specific scanner.

### Image processing

Dual-energy data were processed by the GSI general protocol on the CT workstation (Advantage Windows, version 4.5; GE Healthcare). A region of interest (ROI) was applied over the renal stone viewed on the bone window settings (Figure 1) occupying approximately 50% of the stone area on axial images. The GSI effective Z (GSI  $Z_{\text{eff}}$ ) represents the calculated effective atomic number of the ROI area and forms part of the standard dual-energy ROI data calculated by the GSI software (Figure 2). Attenuation of the ROI area at monochromatic energy 70 keV also forms part of the vendor-specific GSI ROI data (Figure 3). Both these values were obtained from the GSI data exported to a standard spreadsheet.

### Crystallography

The stones extracted via PCNL were sent for analysis to the local National Health Laboratory Service (NHLS) laboratory. Stone composition was determined using infrared



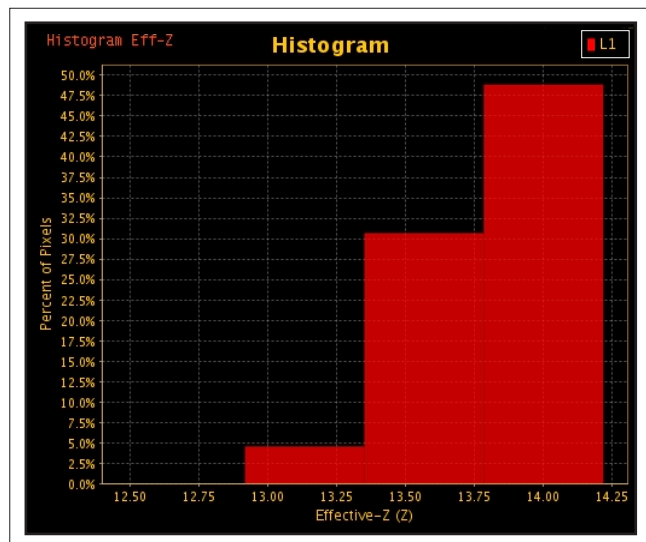
GSI, Gemstone Spectral Imaging.

**FIGURE 1:** Region of interest on a right renal stone viewed in the GSI viewer on bone window settings.

spectroscopy and x-ray diffraction. The  $Z_{\text{eff}}$  value according to stone composition analysis (Calc  $Z_{\text{eff}}$ ) was calculated using Mayneord's equation<sup>14</sup> and then used as the standard against which to compare the GSI  $Z_{\text{eff}}$ .

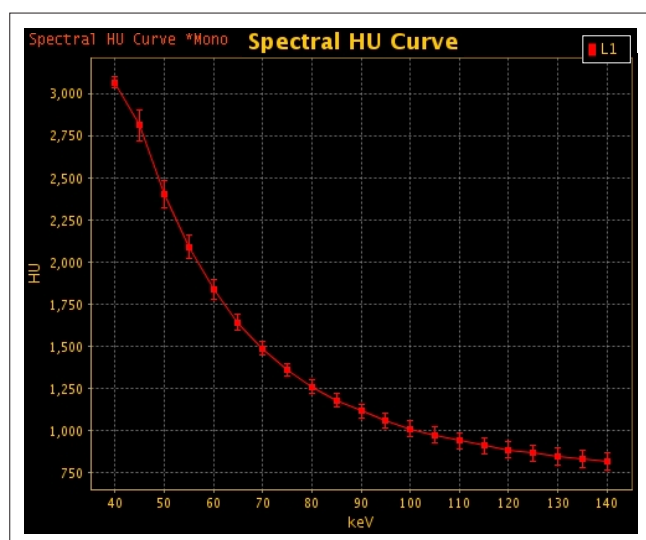
## Statistical analysis

Statistical analysis was performed using SAS/STAT statistical analysis software and Microsoft Excel. Two different strategies were used to evaluate the accuracy of determination of renal stone composition. Firstly, we wanted to determine whether the GSI  $Z_{\text{eff}}$  for each stone was similar to the Calc  $Z_{\text{eff}}$ . The GSI  $Z_{\text{eff}}$  was subtracted from the Calc



$Z_{\text{eff}}$  effective atomic number ROI, region of interest; GSI, Gemstone Spectral Imaging; Z, atomic number.

**FIGURE 2:** Histogram of the  $Z_{\text{eff}}$  ranges of pixels in the ROI. This is displayed in the GSI viewer on the workstation. The average effective Z for the ROI is calculated by the GSI software and represented on a spreadsheet of all GSI data for the specific ROI (not shown here).



HU, Hounsfield units; GSI, Gemstone Spectral Imaging; ROI, region of interest;  $Z_{\text{eff}}$  effective atomic number.

**FIGURE 3:** Stone attenuation (HU) plotted against monochromatic keV, displayed in the GSI viewer on the workstation. Specific attenuation values (HU) for every monochromatic energy from 40 to 140 keV are also provided in the ROI-specific spreadsheet data (not shown). We plotted the stone  $Z_{\text{eff}}$  against the attenuation at monochromatic 70 keV to attempt separating different groups (Figure 4).

$Z_{\text{eff}}$  for each stone to determine the difference (diff\_Z), and the median diff\_Z for all stones was calculated to determine whether the difference between the GSI  $Z_{\text{eff}}$  and Calc  $Z_{\text{eff}}$  was statistically significant. Secondly, we plotted the GSI  $Z_{\text{eff}}$  against the attenuation (HU) at 70 keV for each stone group to determine whether there was good separation between the groups based on the GSI  $Z_{\text{eff}}$ .

## Results

Twenty-five patients were included in the study. Six patients had to be excluded due to PCNL cancellations or insufficient extracted stone fragments for laboratory analysis. Thus only 19 patients with confirmed *ex vivo* renal-stone analysis results were included in the study. The patients' ages ranged from 19 years to 66 years, with a mean age of 45 years. Eleven (57.9%) patients were male.

The laboratory stone compositions, GSI  $Z_{\text{eff}}$ , calculated  $Z_{\text{eff}}$  and attenuation (HU) at 70 keV are listed in Table 1.

The median diff\_Z was 0.82, although the difference between the GSI  $Z_{\text{eff}}$  value and calculated  $Z_{\text{eff}}$  value was not statistically significant, with a 95% confidence interval (CI) of [-0.28; 1.54].

The scatter plot of the GSI  $Z_{\text{eff}}$  of the individual renal stones versus their attenuation at 70 keV demonstrates that uric acid separation from the calcium-containing stones was graphically possible (Figure 4). Both stones with a predominant uric acid component fell below a GSI  $Z_{\text{eff}}$  of 10 and an attenuation of 400 HU at 70 keV.

## Discussion

Knowledge of the chemical composition of urinary tract stones is essential for planning the management of patients.<sup>8</sup> Dual-energy CT is an emerging application for possible *in vivo* characterisation of renal stones, although data on the subject are limited at this stage. This was the first study on *in vivo* renal stone characterisation done in South Africa using the single-source, dual-energy system by GE Healthcare.

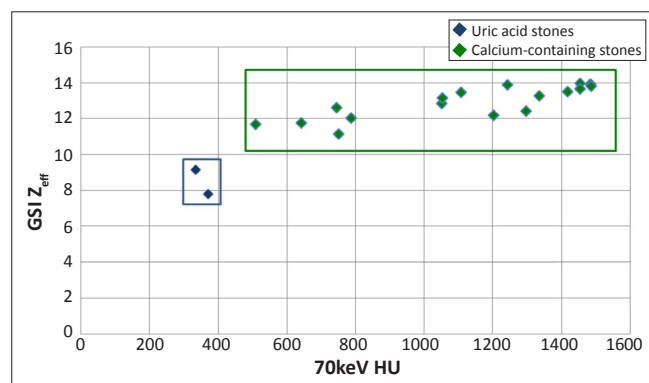
Our results indicate that the GSI  $Z_{\text{eff}}$  measurement can differentiate between uric acid and non-uric acid stones, which was in keeping with the findings of a recent study by Kulkarni et al. on a machine with the same specifications.<sup>10</sup> As found in previous *in vivo* studies,<sup>10,13</sup> we could not accurately differentiate between the different subtypes of calcium stones. In our small study of 19 patients, only two patients had stones with uric acid as major component; the other 17 had calcium-based stones. As we did not encounter any stones of the cystine or struvite group, we could not provide data on the differentiation of these stones from other stone groups.

The polycrystalline composition of our calcium-based stone group complicated the differentiation of stone compositions, which was demonstrated by the inability to separate clearly different stone compositions from one another on the scatter

**TABLE 1:** Composition, effective atomic number and Hounsfield units of urinary tract stones ( $N = 19$ ).

Laboratory stone composition	$n$	Mean GSI $Z_{\text{eff}}$ (range)	Calculated $Z_{\text{eff}}$	Mean HU at 70 keV (range)
Calcium oxalate monohydrate 50%; Calcium oxalate dihydrate 50%	10	12.8 (11.13–13.94)	13.22	1149.69 (508.67–1486.42)
Carbonite apatite 100%	2	13.42 (12.85–13.98)	15.74	1252.46
Carbonite apatite 90%; Calcium oxalate dihydrate 10%	1	13.9	15.47	1243.47
Calcium oxalate monohydrate 65%; Calcium oxalate dihydrate 14%; Uric acid dihydrate 20%	1	11.77	10.56	641.84
Calcium oxalate monohydrate 12%; Carbonite apatite 71%; Uric acid dihydrate 17%	1	12.6	12.79	745.21
Calcium oxalate monohydrate 50%; Carbonite apatite 50%	1	13.26	14.60	1336.21
Calcium oxalate monohydrate 50%; Uric acid dihydrate 50%	1	9.14	10.23	334.36
Calcium oxalate monohydrate 10%; Uric acid dihydrate 90%	1	7.78	7.74	370.97
Calcium oxalate monohydrate 100%	1	13.16	13.45	1053.62

$Z_{\text{eff}}$  effective atomic number; HU, Hounsfield units;  $n$ , number; GSI, Gemstone Spectral Imaging.



GSI, Gemstone Spectral Imaging;  $Z_{\text{eff}}$  effective atomic number; HU, Hounsfield units.

**FIGURE 4:** GSI  $Z_{\text{eff}}$  of individual renal stones versus their attenuation at 70 keV.

plot (Figure 4). Only three (15.8%) of the 19 stones were pure. The single pure calcium oxalate monohydrate (COM) stone had a mean GSI  $Z_{\text{eff}}$  of 13.16, which was very similar to the *in vitro* (13.21) and *in vivo* (13.86) results obtained by Kulkarni et al.<sup>10</sup> in the only published study using similar technology *in vivo*. Their study did not contain carbonite apatite stones<sup>10</sup> and therefore no comparison could be made to this stone type.

Our findings also confirmed that the GSI  $Z_{\text{eff}}$  value in a polycrystalline stone reflects the dominant composition, similar to the findings of Kulkarni et al.<sup>10</sup> Our stone composed of 10% COM and 90% uric acid (UA) had a GSI  $Z_{\text{eff}}$  of 7.78, compared to their value of 7.77 (20% COM and 80% UA stone). This value is close to the GSI  $Z_{\text{eff}}$  value of pure UA *in vivo* (7.3).<sup>10</sup> Similarly, our calcium oxalate 80% and uric acid 20% stone had a GSI  $Z_{\text{eff}}$  of 11.77, compared to their 11.45 (80% COM and 20% UA).<sup>10</sup>

The lack of a statistically significant difference between the GSI  $Z_{\text{eff}}$  and calculated  $Z_{\text{eff}}$  for stone groups in our study, and the similarity in GSI  $Z_{\text{eff}}$  results to other studies using similar technology,<sup>10,12</sup> support GSI  $Z_{\text{eff}}$  accuracy for possible renal stone composition determination in future. It should be noted, however, that no clinically acceptable margins of error have been proposed for  $Z_{\text{eff}}$  values due to the small number of *in*

*vivo* studies on limited stones. In our study, the measured GSI  $Z_{\text{eff}}$  values ranged between 7.78 and 13.98 (11.13 and 13.98 when excluding uric acid-containing stones). This small difference (2.85) in GSI  $Z_{\text{eff}}$  values is likely to make stone differentiation of non-uric acid polycrystalline stones very difficult in the clinical setting, where pure stones appear to be minimal. The polycrystalline stones differ slightly regarding their effective atomic number and any combination of stone constituents can result in a given  $Z_{\text{eff}}$  value.

Large stones are surgically managed by stone fragmentation using shock wave lithotripsy or alternatively by ureteroscopy or PCNL.<sup>5,11</sup> El-Assmy et al.<sup>8</sup> demonstrated that high CT attenuation (> 1000 HU) of a stone is a significant predictor of failure to fragment renal stones by shock wave lithotripsy. Future studies on dual-energy monochromatic attenuation values or GSI  $Z_{\text{eff}}$  values as predictors of failure to fragment renal stones may be of value to refine treatment algorithms.

There were a number of limiting factors in the study. Only a small number of stones were included due to the limited patient cohort. We did not evaluate the effect of stone and patient size on attenuation values, as this was not our primary research question. No stones of cystine or struvite composition were encountered in our study population. Due to insufficient stone fragments for laboratory analysis and PCNL cancellations, six patients had to be excluded from the study.

Continued *in vivo* studies on dual-energy CT renal stone characterisation with larger stone numbers are needed to attempt better differentiation of calcium-based stones and refinement of dual-energy CT protocols.

## Conclusion

Single-source dual-energy CT with GSI in the study accurately distinguished between uric acid and non-uric acid renal stones, but failed to subclassify calcium-based non-uric acid stones. Mixed uric acid and non-uric acid stones demonstrate characteristics of the dominant component.

The effective atomic number of renal stones determined by means of dual-energy CT shows no significant difference to the calculated effective number using the laboratory stone composition. Despite limited stone numbers, effective atomic number calculation with dual-energy CT shows promise in determination of renal stone composition.

## Acknowledgements

The authors acknowledge the personnel of the Department of Urology and the radiographers at Universitas Academic Hospital for assistance; the personnel of the Unit for Interventional Radiology for extraction of the renal stones; Mr Cornel van Rooyen, Department of Biostatistics, Faculty of Health Sciences, University of the Free State, for statistical analysis of data; and Dr Daleen Struwig, medical writer, Faculty of Health Sciences, University of the Free State, for technical and editorial preparation of the manuscript.

## Competing interests

The authors declare that they have no financial or personal relationship(s) that may have inappropriately influenced them in writing this article. The authors are not employees of GE Healthcare and no funding was received from GE Healthcare for the study.

## Authors' contributions

J.H.C. (University of the Free State) was the principal investigator and wrote the manuscript. W.S.H. (University of the Free State) made conceptual contributions and was involved with manuscript editing.

## References

1. Eliahou R, Hidas G, Duvdevani M, Sosna J. Determination of renal stone composition with dual-energy computed tomography: An emerging application. *Semin Ultrasound CT MR*. 2010;31(4):315–320. <http://dx.doi.org/10.1053/j.sult.2010.05.002>, PMID 20691932
2. Rodgers A. The riddle of kidney stone disease: Lessons from Africa. *Urol Res*. 2006;34(2):92–95. <http://dx.doi.org/10.1007/s00240-005-0017-1>, PMID 16555110
3. Schubert G. Stone analysis. *Urol Res*. 2006;34(2):146–150. <http://dx.doi.org/10.1007/s00240-005-0028-y>, PMID 16477427
4. Saita A, Bonaccorsi A, Motta M. Stone composition: Where do we stand? *Urol Int*. 2007;79(suppl. 1):16–19. <http://dx.doi.org/10.1159/000104436>, PMID 17726347
5. Tseng TY, Stoller ML. Medical and medical/urologic approaches in acute and chronic urologic stone disease. *Med Clin North Am*. 2011;95(1):169–177. <http://dx.doi.org/10.1016/j.mcna.2010.08.034>, PMID 21095420
6. Hidas G, Eliahou R, Duvdevani M, et al. Determination of renal stone composition with dual-energy CT: In vivo analysis and comparison with x-ray diffraction. *Radiology*. 2010;257(2):394–401. <http://dx.doi.org/10.1148/radiol.10100249>, PMID 20807846
7. Catalano O, Nunziata A, Altei F, Siani A. Suspected ureteral colic: Primary helical CT versus selective helical CT after unenhanced radiography and sonography. *Am J Roentgenol*. 2002;178(2):379–387. <http://dx.doi.org/10.2214/ajr.178.2.1780379>, PMID 11804898.
8. El-Assmy A, Abou-el-Ghar ME, el-Nahas AR, Refaie HF, Sheir KZ. Multidetector computed tomography: Role in determination of urinary stones composition and disintegration with extracorporeal shock wave lithotripsy – An in vitro study. *Urology*. 2011;77(2):286–290. <http://dx.doi.org/10.1016/j.urology.2010.05.021>, PMID 20719366
9. Li X, Zhao R, Liu B, Yu Y. Gemstone spectral imaging dual-energy computed tomography: A novel technique to determine urinary stone composition. *Urology*. 2013;81(4):727–730. <http://dx.doi.org/10.1016/j.urology.2013.01.010>, PMID 23453078
10. Kulkarni NM, Eisner BH, Pinho DF, Joshi MC, Kambadakone AR, Sahani DV. Determination of renal stone composition in phantom and patients using single-source dual-energy computed tomography. *J Comput Assist Tomogr*. 2013;37(1):37–45. <http://dx.doi.org/10.1097/RCT.0b013e3182720f66>, PMID 23321831
11. Joshi MC, Langan DA, Sahani DS, et al. Effective atomic number accuracy for kidney stone characterization using spectral CT. Bellingham, Washington: International Society for Optical Engineering, 2010.
12. Li XH, Zhao R, Liu B, Yu YQ. Determination of urinary stone composition using dual-energy spectral CT: Initial in vitro analysis. *Clin Radiol*. 2013;68(7):e370–e377. <http://dx.doi.org/10.1016/j.crad.2012.11.022>, PMID 23535316
13. Manglaviti G, Tresoldi S, Guerrer CS, et al. In vivo evaluation of the chemical composition of urinary stones using dual-energy CT. *Am J Roentgenol*. 2011;197(1):W76–W83. <http://dx.doi.org/10.2214/AJR.10.5217>, PMID 21700999
14. Goodsitt MM, Christodoulou EG, Larson SC. Accuracies of the synthesized monochromatic CT numbers and effective atomic numbers obtained with a rapid kVp switching dual energy CT scanner. *Med Phys*. 2011;38(4):2222–2232. <http://dx.doi.org/10.1118/1.3567509>, PMID 21626956